

Comparison of Transfer Matrix (T-matrix) and Coupling of Modes in Time (CMT) Models of Coupled Microring Resonator Filters

Miljan Dašić

Student of the first level studies

Faculty of Electrical Engineering, University of Belgrade,
Belgrade, Serbia

miljandasic@yahoo.com

Abstract—The aim of this paper is to use theoretical models of coupled microring resonator filter to show its operation and to apply those calculations in order to maximize drop port power. Coupled microring resonators are one of fundamental elements in photonic devices. They have good resonator characteristics useful for filter applications, because arbitrary -3dB bandwidth and FSR(Free Spectral Range) are easily designed. Theoretical models include T-matrix (Transfer Matrix) and CMT (Coupling of Modes in Time). A comparison of those models is shown. CMT model is applied in optimization of transmission to the drop port.

Key words-model; transfer matrix; coupling of modes in time; microring; resonator; filters;

I. INTRODUCTION

INTEGRATED silicon based photonics has many promising applications in optical telecommunications, optoelectronics and optical signal processing [1]–[4]. The integration of silicon photonics and electronic circuits offers the prospect of low energy devices, circuits and systems for applications including on-chip and processor-to-memory interconnects [3], [4], as well as photonic analog-to-digital converters [5]. Other applications include nonlinear and quantum devices for applications in quantum information and computing [6]. An important photonic device, and one of the earliest concepts realized in integrated photonics, is the resonant channel add-drop filter. Microring resonators are particularly well suited for add-drop filter applications [7], [8] because of their traveling wave structure that allows for a natural separation of the four ports (in, through, drop, add).

II. TRANSFER MATRIX MODEL

In the Fig. 1. schematic drawing of a ring resonator coupled to two bus waveguides is shown. In transfer matrix model we have two linear systems. First one has optical signal amplitude inputs of a_1 and a_2 , and outputs of b_1 and b_2 . It represents coupling of the first bus to the ring with

coupling coefficient of k_i , while the other linear system represents coupling of the second bus to the ring with

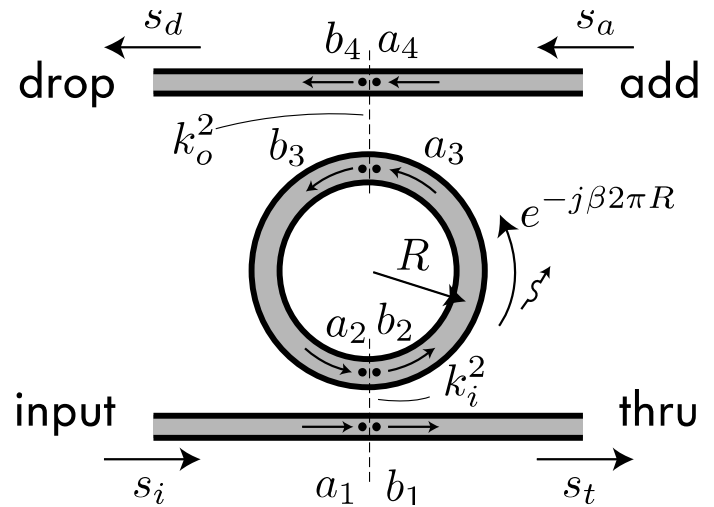


Fig. 1. Schematic of a microring-resonator add-drop filter showing the parameters used in the T matrix model

coupling coefficient of k_0 , where optical amplitude inputs are a_3 and a_4 while outputs are b_3 and b_4 . In transfer matrix model we want to solve next matrix equation

$$\begin{pmatrix} b_4 \\ b_1 \end{pmatrix} = \bar{\bar{T}} \times \begin{pmatrix} a_4 \\ a_1 \end{pmatrix} = \begin{pmatrix} T_{11} & T_{12} \\ T_{21} & T_{22} \end{pmatrix} \times \begin{pmatrix} a_4 \\ a_1 \end{pmatrix} \quad (1)$$

Optical signals a_1 and a_2 are coming from input ports, b_1 leaves the system at through port and optical signal b_4 leaves the system at drop port. The goal is to determine transfer matrix $\bar{\bar{T}}$. We solve it using next three matrix equations. First two stand for the linear systems that model couplings of the buses to the ring while third one is about the phase constraint for the signals propagating in the microring resonator [2], [9].

$$\begin{pmatrix} b_1 \\ b_2 \end{pmatrix} = \overset{=}{t} \times \begin{pmatrix} a_1 \\ a_2 \end{pmatrix} = \begin{pmatrix} \sqrt{1-k_i} - j\sqrt{k_i} \\ -j\sqrt{k_i}\sqrt{1-k_i} \end{pmatrix} \times \begin{pmatrix} a_1 \\ a_2 \end{pmatrix} \quad (2)$$

$$\begin{pmatrix} b_3 \\ b_4 \end{pmatrix} = \overset{=}{\tau} \times \begin{pmatrix} a_3 \\ a_4 \end{pmatrix} = \begin{pmatrix} \sqrt{1-k_o} - j\sqrt{k_o} \\ -j\sqrt{k_o}\sqrt{1-k_o} \end{pmatrix} \times \begin{pmatrix} a_3 \\ a_4 \end{pmatrix} \quad (3)$$

$$\begin{pmatrix} a_3 \\ a_2 \end{pmatrix} = \begin{pmatrix} e^{-j\beta\pi R} 0 \\ 0 e^{-j\beta\pi R} \end{pmatrix} \times \begin{pmatrix} b_2 \\ b_3 \end{pmatrix} \quad (4)$$

In Eq. 4 j is imaginary one, $\beta\pi R$ is the product of propagation constant and half of the circumference of the ring and term R is inner radius of the ring. The expression for beta is

$$\beta = n_g \times \frac{2\pi}{\lambda} \quad (5)$$

where n_g is group refractive index. We use notation:

$$\overset{=}{t} = \begin{pmatrix} t_{11} & t_{12} \\ t_{21} & t_{22} \end{pmatrix} \quad (6)$$

$$\overset{=}{\tau} = \begin{pmatrix} \tau_{11} & \tau_{12} \\ \tau_{21} & \tau_{22} \end{pmatrix}$$

When matrix equations are written in developed form, we obtain

$$\begin{aligned} b_1 &= t_{11}a_1 + t_{12}a_2 \\ b_2 &= t_{21}a_1 + t_{22}a_2 \\ b_3 &= \tau_{11}a_3 + \tau_{12}a_4 \\ b_4 &= \tau_{21}a_3 + \tau_{22}a_4 \end{aligned} \quad (7)$$

Together with the phase constraints

$$\begin{aligned} a_3 &= b_2 \times e^{-j\beta\pi R} \\ a_2 &= b_3 \times e^{-j\beta\pi R} \end{aligned} \quad (8)$$

The algorithm is to solve Eq. 7.4 for a_3 and to obtain b_2 in terms of a_4 and b_4 using Eq. 8.1. Then plug in a_3 to Eq. 7.3 which leads to an expression of b_3 in terms of (a_4, b_4) . We were using Eq. 8.1, Eq. 7.3 and Eq. 7.4. In similar way using Eq. 8.2, Eq. 7.1 and Eq. 7.2 we solve a_2 and b_2 in terms of (a_1, b_1) . Then we have to combine expressions obtained by this separate solvings using

constraint equations (Eq. 8.1 and Eq. 8.2) which leads to this solution

$$\begin{aligned} b_4 &= T_{11}a_4 + T_{12}a_1 \\ b_1 &= T_{21}a_4 + T_{22}a_1 \end{aligned} \quad (9)$$

like in Eq. 1, where expressions for transfer matrix elements are

$$T_{11} = \frac{\tau_{22} + e^{-j2\beta\pi R} t_{22} (\tau_{12}\tau_{21} - \tau_{11}\tau_{22})}{(1 - e^{-j2\beta\pi R} \tau_{11}t_{22})}$$

$$T_{12} = \frac{e^{-j\beta\pi R} \tau_{21}t_{21}}{(1 - e^{-j2\beta\pi R} \tau_{11}t_{22})} \quad (10)$$

$$T_{21} = \frac{e^{-j\beta\pi R} t_{12}\tau_{12}}{(1 - e^{-j2\beta\pi R} \tau_{11}t_{22})}$$

$$T_{22} = \frac{t_{11} + e^{-j2\beta\pi R} \tau_{11} (t_{12}t_{21} - t_{11}t_{22})}{(1 - e^{-j2\beta\pi R} \tau_{11}t_{22})}$$

Here T_{12} represents normalized drop port power and T_{22} represents normalized through port power. Now we apply those expressions from Eq. 10 to calculate spectral response of a filter made of two bus waveguides that are coupled to the microring-resonator. We have chosen free spectral range of 2 THz and -3dB bandwidth of 40 GHz. It is known that free spectral range of a microring-resonator is determined by ring's radius [2].

$$FSR = \frac{c}{2\pi R n_g} \Rightarrow R = \frac{c}{2\pi n_g FSR} \quad (11)$$

Taking the Eq. 12 from reference [1] and using

$$\lambda = \frac{c}{f} \Rightarrow |d\lambda| = \frac{c}{f^2} df \quad (12)$$

gives us the relation for -3dB bandwidth

$$\pi \cdot \Delta f_{-3dB} = k^2 \cdot 2FSR \quad (13)$$

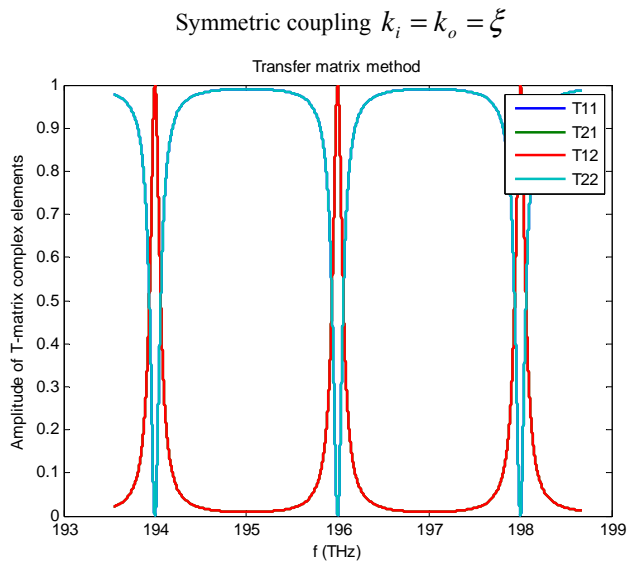
Therefore we define normalized coupling

$$\xi = \sqrt{\frac{\pi \times \Delta f_{-3dB}}{2FSR}} \quad (14)$$

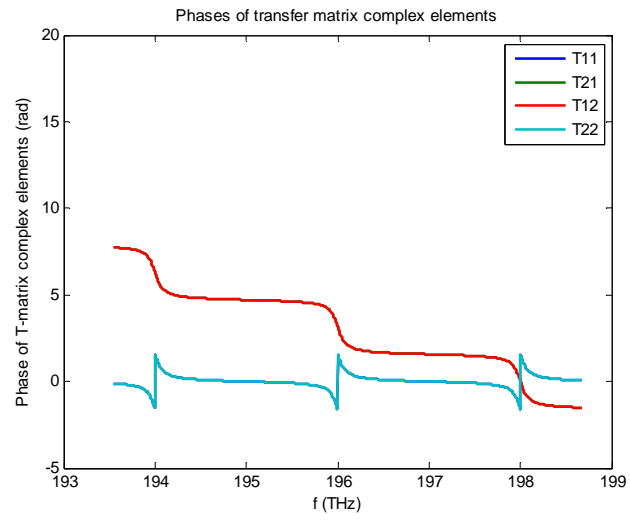
Delay in group time is calculated using this formula

$$t_g = -\frac{1}{2\pi} \frac{d\Phi}{df} \quad (15)$$

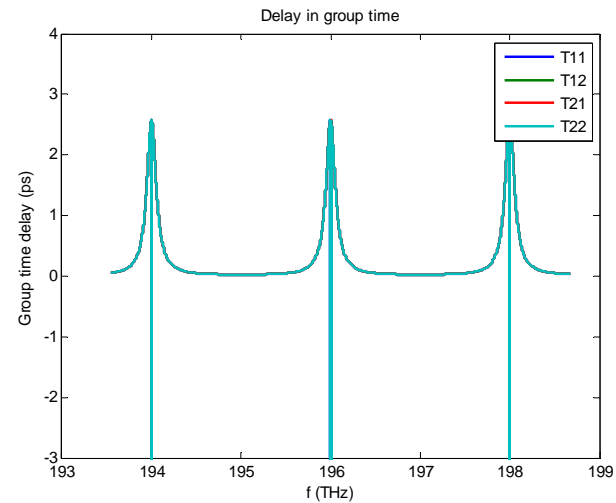
where Φ is the phase and f is the frequency.



(a)

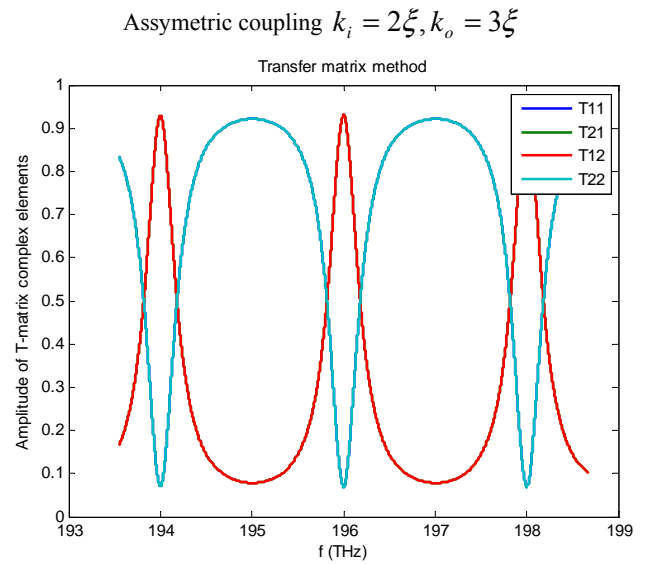


(b)

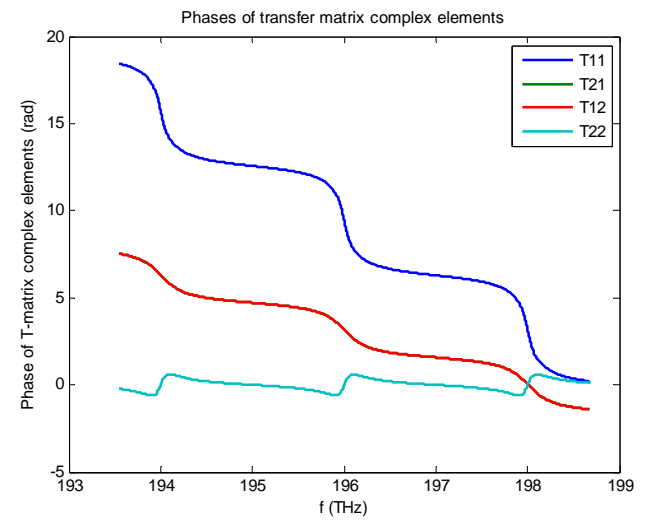


(c)

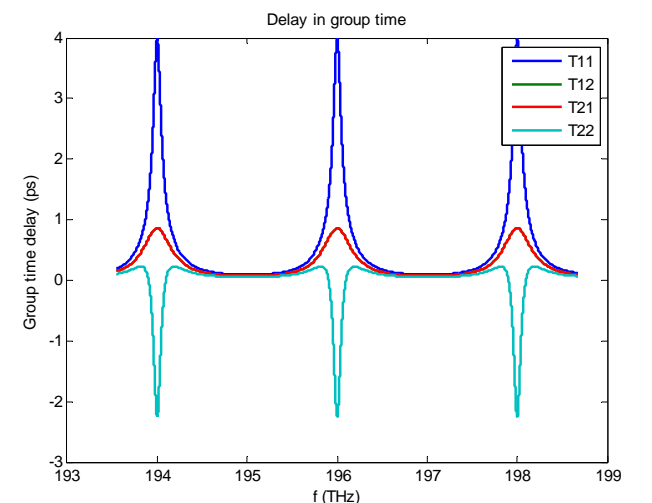
Fig. 2. Frequency spectra of T-matrix elements' amplitude, phase and group time delay - (a), (b), (c)



(a)



(b)



(c)

Fig. 3. Frequency spectra of T-matrix elements' amplitude, phase and group time delay - (a), (b), (c)

In Fig. 2 and Fig. 3 frequency spectra of T-matrix elements' amplitude, phase and group time delay are given, in symmetric and chosen asymmetric case, respectively. We can notice that symmetric coupling affords 100% transmission to the drop port. In the phase and group time delay plots we can notice differentiation of the bus lines, caused by the asymmetric coupling.

III. COUPLING OF MODES IN TIME (CMT) MODEL

Coupled-mode theory in time (CMT) provides a simple model that affords all necessary physics of the resonant add-drop filter problem, including resonance, loss and coupling to input and output ports [1,2,6]. The system of equations that describes a single-resonator filter excited by a monochromatic input wave at angular frequency ω is

$$\begin{aligned} \frac{d}{dt} a(t) &= j\omega a(t) = (j\omega_0 - r)a(t) - j\sqrt{2r_e} s_i(t) \\ s_i(t) &= s_i(t) - j\sqrt{2r_e} a(t) \\ s_d(t) &= -j\sqrt{2r_d} a(t) \end{aligned} \quad (16)$$

where $a(t)$ is energy amplitude of the ring resonant mode, s_i , s_s , s_d , are the power-normalized amplitudes of input, through and drop port waves [2]. With input wave s_i incident, some excitation is picked up by the resonator, and the remaining field interferes with that leaving the resonator in the through port and is carried away by through-port wave s_t . The energy stored in the resonator is $|a(t)|^2$ and according to Eqs. (16) the energy amplitude $a(t)$ decays at a total rate r , comprising decay rates describing external coupling to the input port, r_e , to the drop port, r_d , and to loss mechanisms, r_o :

$$r = r_e + r_d + r_o \quad (17)$$

The coupling rates r_e and r_d are determined in the evanescent-coupling geometry in Fig. 8 by the size of the ring-waveguide coupling gaps [1,9]. The decay rates are related to decay time constants as $r_i = 1/\tau_i$, for $i = \{e, d, o\}$. Since τ is a field time constant, the associated photon lifetime of the resonant cavity (which measures decay of intensity) is $\tau/2$.

The through-port and drop-port responses of the device can be found from Eqs. (16) as

$$\left| \frac{s_t}{s_i} \right|^2 = \frac{(\omega - \omega_0)^2 + (r_0 + r_d - r_e)^2}{(\omega - \omega_0)^2 + (r_0 + r_d + r_e)^2} \quad (18)$$

$$\left| \frac{s_d}{s_i} \right|^2 = \frac{4r_e r_d}{(\omega - \omega_0)^2 + r^2} \quad (19)$$

The drop-port response is Lorentzian, with a full 3dB bandwidth $\Delta\omega_{3dB} = 2r$.

Unlike a full scattering model (T matrix model) using transfer matrices, the CMT model addresses only one resonant mode of the ring and does not include geometry information that can define a free spectral range (FSR).

Resonant frequencies are determined by the resonant condition

$$f_m = m \frac{c}{2\pi R n_{eff}} \quad (20)$$

where c is the speed of light in vacuum, R is the ring resonator radius, and n_{eff} is the (frequency dependent) effective index of the guided mode. The FSR is given by

$$\Delta f_{FSR} = \frac{c}{2\pi R n_g} \quad (21)$$

where n_g is group effective index of the guided mode.

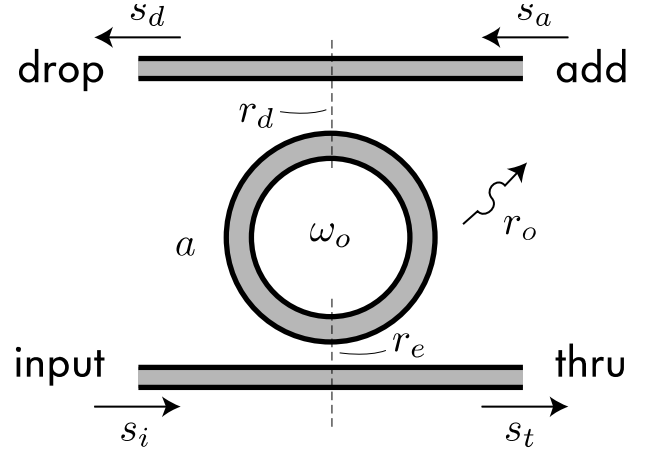


Fig. 4. Schematic of a single microring-resonator add-drop filter showing the parameters used in the CMT model.

IV. CORRESPONDENCE OF CMT AND T-MATRIX MODELS

We have derived T-matrix and CMT models of coupled microring resonator filters. Now we will compare those models. In Fig. 5 we show wavelength spectra of amplitude in linear and db scale. The task is to connect coupling coefficients k_i, k_o from T-matrix model with decay rates r_e, r_d . There is a direct relation [1]

$$r_m = 2k_n^2 \times FSR \quad (22)$$

for $m = \{e, d\}$ and $n = \{i, o\}$. Using normalized couplings from Eq. (14) we obtain expression for decay rates as

$$r = \pi \cdot \Delta f_{-3dB} \quad (23)$$

We are showing the results of comparison for symmetric coupling, with zero losses. One disadvantage of T-matrix model is that it does not model losses while CMT model includes losses. On the other side, T-matrix shows free spectral range and multiple resonances while CMT model has only one resonant wavelength. In Fig. 5(b) we can

notice that deviation of CMT Lorentzian from T-matrix trace is bigger on dB scale than on linear scale in Fig.5 (a).

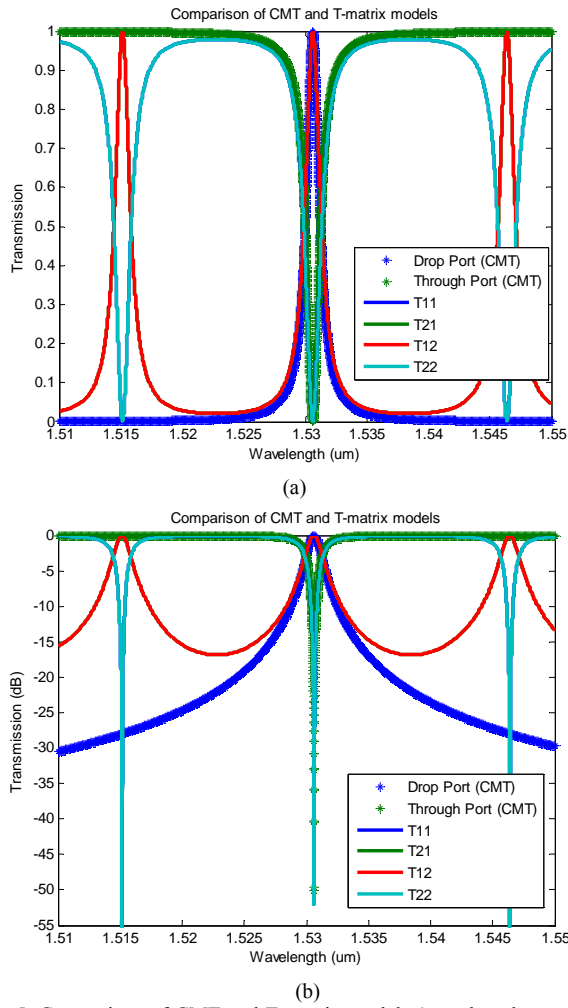


Fig. 5. Comparison of CMT and T-matrix models (wavelength spectra of amplitude) linear (a) and dB scale (b)

V. OPTIMAL AND CRITICAL COUPLING

We apply CMT model in order to optimize drop port transmission. Fixing the bandwidth means fixing the total rate r , according to Eq. (17) and, together with a fixed loss rate, there is only one degree of freedom left. Taking the first derivative of Eq. (19) in respect to r_e and setting this to zero gives

$$r_e = r_d = \frac{r - r_0}{2} \quad (24)$$

From setting Eq. (18) to zero on-resonance, we derive the couplings of critically coupled filter

$$r_e = r_d + r_0 \quad (25)$$

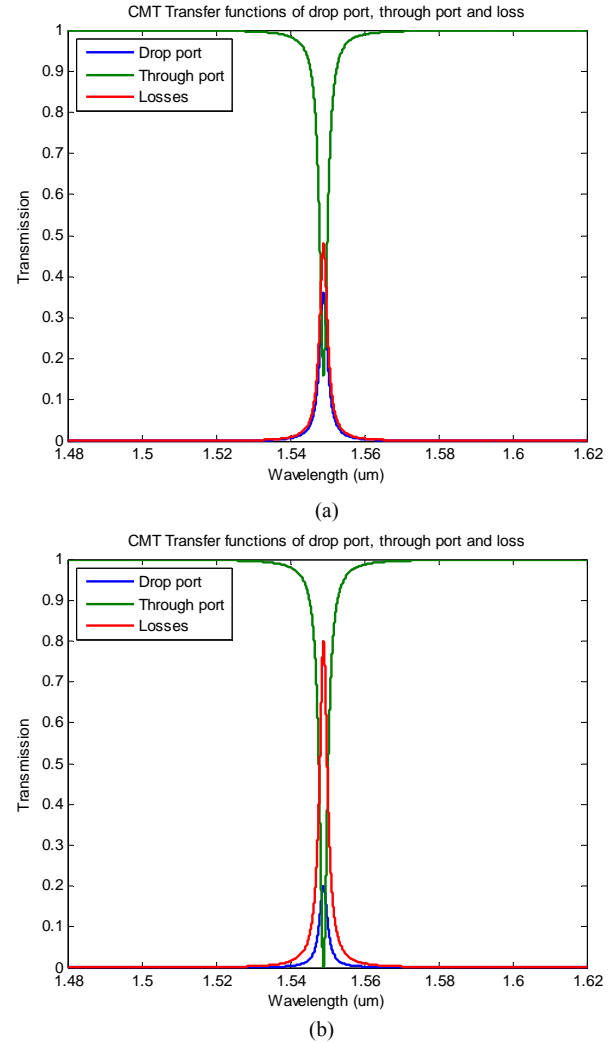


Fig. 6. CMT transmission (drop port, through port and losses) in optimally and critically coupled filters – (a), (b)

In Fig. 6 transmission spectra of through and drop port is given for optimally and critically coupled filters. A comparison of the transmission efficiency of the optimal symmetric [Eq. (24)] and critical coupling [Eq. (25)] designs is given in Fig. 7, showing that the symmetric design is indeed optimal for maximizing dropped on-resonant power. We define a normalized bandwidth, α , by normalizing the 3dB bandwidth Δf_{3dB} by the intrinsic linewidth Δf_o due to the loss rate r_o , i.e. loss Q, Q_o . Substitution of the solutions of Eq. (24) and Eq. (25) into Eq. (19) provides the normalized efficiency of the symmetric and critically coupled designs given in Eq. (26).

$$\left| \frac{s_d}{s_i} \right|_{optimal}^2 = \left(1 - \frac{1}{\alpha} \right)^2 \quad (26)$$

$$\left| \frac{s_d}{s_i} \right|_{critical}^2 = 1 - \frac{2}{\alpha}$$

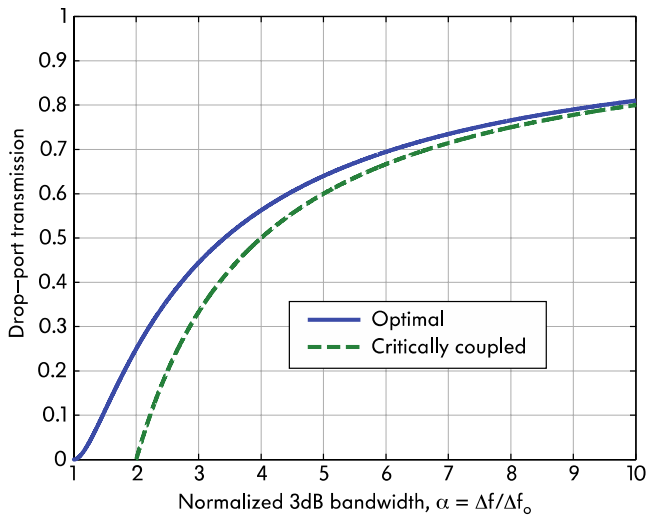


Fig. 7. Minimizing the impact of loss on a single filter stage: comparison of symmetric (optimal) and critically coupled single-ring filter designs for different normalized bandwidths, (ratio of total bandwidth to loss-limited, intrinsic bandwidth). Ref. [12]

TABLE I
MINIMUM NORMALIZED BANDWIDTH FOR 3DB DROP-PORT POWER

Symmetric coupling	Critical coupling
$\frac{\sqrt{2}}{\sqrt{2}-1} \approx 3,412$	4

VI. CONCLUSION

Transfer matrix model of a photonic microring-resonator channel add-drop filter has been solved and applied to design a filter with chosen free spectral range (FSR) and -3dB bandwidth (Δf_{3dB}). The results of those calculations are given for symmetric and asymmetric coupling. CMT model was solved and applied in order to maximize drop port power of a single ring filter. We have determined how to choose optimal couplings and then compared this to the case of critical coupling. This comparison is useful in the design process to determine the narrowest bandwidth that supports a desired transmission to the drop port, or the maximum transmission achievable at a certain bandwidth, given known linear losses. Fig. 7 and Eqs. (26) show that the optimum symmetric design has a minimum bandwidth limit of Δf_0 , while the critically coupled design has a minimum bandwidth of $2\Delta f_0$. In the limit of a large bandwidth α , the loss plays a negligible role and the two solutions can be verified by a first-order Taylor series expansion of Eqs. (26) to be equal.

ACKNOWLEDGEMENT

Author is very thankful for all the support of professor Miloš A. Popović, who was the supervisor of the research presented in this paper. First of all, he gave me a great opportunity to work as a research intern in his Nanophotonic Systems Laboratory at Electrical, Computer and Energy Engineering Department, University of Colorado Boulder, United States of America. His ideas and comments guided me through this research. Many thanks to all the people from our group - Savvy, Chris, Kareem, Mark, Cale, Jeff and Yangyang whose support and help made my work more efficient.

REFERENCES

- [1] B. E. Little, S. T. Chu, H. A. Haus, J. Foresi and J.-P. Laine, "Microring Resonator Channel Dropping Filters", *Journal of Lightwave Technology*, June 1997, vol. 15, No. 6
- [2] H. A. Haus, "Waves and Fields in Optoelectronics", Englewood Cliffs, NJ: Prentice-Hall, 1984.
- [3] J.S. Orcutt, B. Moss, C. Sun, J. Leu, M. Georgas, J. Shainline, E. Zraggen, H. Li, J. Sun, M. Weaver, S. Urosevic, M.A. Popovic, R.J. Ram and V.M. Stojanovic, "An Open Foundry Platform for High-Performance Electronic-Photonic Integration", *Optics Express* 20, 12222-12232 (2012).
- [4] H. A. Haus and Y. Lai, "Narrow-band optical channel-dropping filter", *Journal of Lightwave Technol.* Jan. 1992., vol. 10
- [5] A. Khilo et al., "Photonic ADCs: Overcoming the Electronic Jitter Bottleneck", *Optics Express* 20, pp. 4454-4469 (2012).
- [6] S. Clemmen, K. Phan Huy, et al., "Continuous wave photon pair generation in silicon-on-insulator waveguides and ring resonators", *Optics Express* 17, 16558-16570 (2009).
- [7] B. E. Little, J. S. Foresi, G. Steinmeyer, E. R. Thoen, S. T. Chu, H. A. Haus, E. P. Ippen, L. C. Kimerling, and W. Greene, "Ultra-compact Si - SiO₂ microring resonator optical channel dropping filters", *IEEE Photon. Technol. Lett.*, vol. 10, pp. 549-551, Apr. 1998.
- [8] C. Manolatou, M. J. Khan, Shanhui Fan, Pierre R. Villeneuve, H. A. Haus, *Life Fellow, IEEE*, and J. D. Joannopoulos, "Coupling of Modes Analysis of Resonant Channel Add-Drop Filters", *IEEE Journal of Quantum Electronics*, vol. 35, no. 9, September 1999.
- [9] A. Yariv and P. Yeh, "Photonics - Optical Electronics in Modern Communications", New York Oxford, Oxford University Press, 2007.
- [10] Andreas Vörckel, Mathias Mönster, Wolfgang Henschel, Peter Haring Bolivar, and Heinrich Kurz, "Asymmetrically Coupled Silicon-On-Insulator Microring Resonators for Compact Add-Drop Multiplexers", *IEEE Photonics Technology Letters*, vol. 15, no. 7, July 2003
- [11] M.A. Popović, "Sharply-defined optical filters and dispersionless delay lines based on loop-coupled resonators and 'negative' coupling," in Conference on Lasers and Electro-Optics(CLEO), 2007
- [12] M. Dašić and M.A. Popović, "Minimum Drop Loss Design of Microphotonic Microring Resonator Channel Add-Drop Filters", Telecommunications Forum (TELFOR) 2012, Belgrade, Serbia